Ultrasonics 73 (2017) 262–270

Contents lists available at ScienceDirect

Ultrasonics

journal homepage: www.elsevier.com/locate/ultras

Directivity analysis of meander-line-coil EMATs with a wholly analytical method

Yuedong Xie [a], Zenghua Liu [b], Liyuan Yin [c], Jiande Wu [c], Peng Deng [b], Wuliang Yin [a,*]

[a] School of Electrical and Electronic Engineering, University of Manchester, Manchester, United Kingdom
[b] College of Mechanical Engineering and Applied Electronics Technology, Beijing University of Technology, Beijing 100124, China
[c] School of Information Engineering and Automation, Kunming University of Science and Technology, Kunming, China

ARTICLE INFO

Article history:
Received 6 May 2016
Received in revised form 16 August 2016
Accepted 17 September 2016
Available online 17 September 2016

Keywords:
Electromagnetic acoustic transducers (EMATs)
Rayleigh waves
Modelling and simulation
Analytical solutions
Beam directivity

ABSTRACT

This paper presents the simulation and experimental study of the radiation pattern of a meander-line-coil EMAT. A wholly analytical method, which involves the coupling of two models: an analytical EM model and an analytical UT model, has been developed to build EMAT models and analyse the Rayleigh waves' beam directivity. For a specific sensor configuration, Lorentz forces are calculated using the EM analytical method, which is adapted from the classic Deeds and Dodd solution. The calculated Lorentz force density are imported to an analytical ultrasonic model as driven point sources, which produce the Rayleigh waves within a layered medium. The effect of the length of the meander-line-coil on the Rayleigh waves' beam directivity is analysed quantitatively and verified experimentally.

1. Introduction

A variety of non-destructive testing (NDT) techniques are available in industries, such as radiographic testing (RT), magnetic particle testing (MPT), eddy current methods, magnetic flux leakage (MFL) and ultrasonic methods [1–5]. Due to its advantages of good penetration depth and mechanical flexibility, the piezoelectric ultrasonic method is widely used for thickness measurement, flaw evaluation and material characterization [6–11]. The transducer frequently used for the conventional ultrasonic non-destructive testing is piezoelectric ceramics or crystals [10–12]. However, one primary disadvantage of the piezoelectric ultrasonic testing is the need to have good sonic contact with the test piece, typically by means of a couplant for acoustic impedance matching [13]. Because an EMAT generates ultrasonic waves directly into the testing piece instead of coupling through the transducer, it has advantages in applications where surface contact is not possible or desirable [14,15]. Another attractive feature of EMAT is that a variety of waves modes can be produced based on different combinations of coils and magnets [16,17].

There are two EMAT interactions which can produce ultrasound: the magnetostriction mechanism and the Lorentz force mechanism; both the magnetostriction mechanism and the Lorentz force mechanism are for ferromagnetic materials while only the Lorentz force mechanism is for conductive metallic materials [16,18,19]. In this paper, only EMAT based on Lorentz force mechanism to generate Rayleigh waves is discussed. As shown in Fig. 1, an EMAT system consists basically of a coil carrying an alternating current, a permanent magnet providing a large static magnetic field, and the test piece. In this work, the test piece used is an aluminium plate, which is mainly affected by Lorentz force mechanism, so magnetostriction is not considered. The Lorentz force mechanism is: the coil induces eddy currents **J** in the surface layers of the testing material, and the interaction between the static magnetic field **B** and eddy currents **J** produces a Lorentz stress **F** based on Eq. (1), which in turn generates ultrasound waves propagating within the testing sample.

$$\mathbf{F} = \mathbf{J} \times \mathbf{B} \tag{1}$$

Considerable works were reported on the electromagnetic acoustic transducers (EMATs) simulation, which contained the electromagnetic model and the ultrasonic model [20–23]. In addition, significant works were reported on the effect of parameters, such as the dimension of the coil, the dimension of the magnet, and the lift-off, on the EMATs efficiency for the optimal design of EMATs [24–27]. Because 3-D modelling has a high demand of the computer capacity and requires significant running time, most of the previous work were 2-D simulation focusing on the x-y plane

---

* Corresponding author.
E-mail address: wuliang.yin@manchester.ac.uk (W. Yin).

http://dx.doi.org/10.1016/j.ultras.2016.09.016
0041-624X/

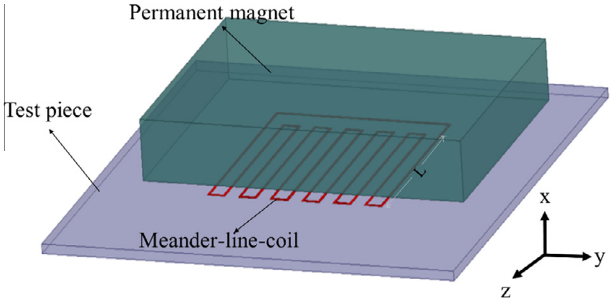

Fig. 1. The configuration of a typical meander-line-coil EMAT.

(i.e. vertical plane) of the material. The orientation of the coordinate system is shown in Fig. 1, and all of the subsequent simulations are based on this coordinate system. Two examples of the 2-D modelling methods for the *x-y* plane of the material have been detailed in [28,29], however, there is little research on the Rayleigh waves' beam directivity on the surface of the material, that is, the *y-z* plane of the material [30].

Consequently, this paper proposes a wholly analytical modelling method to study the Rayleigh waves' beam directivity on the surface of the material. This method involves the coupling of two models: an analytical electromagnetic (EM) model and an analytical ultrasonic (UT) model. The analytical EM model is used to calculate Lorentz force density, which then feed through to the analytical ultrasonic model to study the Rayleigh waves' beam directivity. In addition, the application of this model to the quantitative evaluation of the effect of the length of the meander-line-coil ("*L*" in Fig. 1) was conducted, and experiments were carried out to validate the simulation results.

2. EMAT modelling

In this work, the test piece used is an aluminium plate with a dimension of 600 mm × 600 mm × 25 mm; the coil used is a meander-line-coil with a dimension of 30 mm × 34.163 mm × 0.035 mm; the permanent magnet used is NdFeB35, whose size is 60 mm × 60 mm × 25 mm. The operation frequency is 483 kHz, and the skin depth calculated is 0.117 mm. The velocity of Rayleigh waves used in the aluminium plate is 2.93 mm/μs, so the spacing between two adjacent lines of the meander-line-coil is 3.03 mm, which is equalling to one half of the Rayleigh waves' wavelength, to form the constructive interference. The meander-line-coil carries an alternating current with the peak of 5 A, and the lift-off of the meander-line-coil is 1 mm.

2.1. EM simulation

2.1.1. Adapted analytical solution

The analytical EM solution is adapted from the classic Deeds and Dodd solution, which was originally for the circular coil. This adapted analytical solution proposed by authors has been published in [28]; a brief introduction is presented here. The governing equations for the eddy current phenomena is shown in Eqs. (2)–(4), where **A** is the magnetic vector potential, μ, σ and ε are the permeability, conductivity and permittivity of the material respectively, **I** is the applied current density, ω is the angular frequency of the applied alternating current, **E** is the electric field, and **J** is the induced eddy current [31].

$$\nabla^2\mathbf{A} = -\mu\mathbf{I} + \mu\sigma\frac{\partial\mathbf{A}}{\partial t} + \mu\varepsilon\frac{\partial^2\mathbf{A}}{\partial t^2} + \mu\nabla\left(\frac{1}{\mu}\right) \times (\nabla \times \mathbf{A}) \tag{2}$$

$$\mathbf{E} = -j\omega\mathbf{A} \tag{3}$$

$$\mathbf{J} = \sigma\mathbf{E} \tag{4}$$

For a circular coil with a rectangular cross-section over a layered conductor [14], provided the final analytical solutions for the vector potential calculation, which can be extended to calculate other electromagnetic induction phenomenon. Assuming the conductor only has one layer (as shown in Fig. 2), the solutions can be simplified as:

$$\mathbf{A}(y,x) = \mu_0\mathbf{I}\int_0^\infty \frac{1}{a^2}\left(\int_{ar_1}^{ar_2}\gamma J_1(\gamma)d\gamma\right)J_1(ay)\left(e^{-al} - e^{-a(l+h)}\right)\frac{e^{(2a_1x)}}{(a+a_1)}da \tag{5}$$

$$a_1 = \sqrt{a^2 + j\omega\mu_1\sigma_1} \tag{6}$$

where $\mathbf{A}(y,x)$ is the vector potential within the conductor, μ_0 is the permeability of air, **I** is the applied current density, γ and a are the integration variables, r_1 and r_2 are the inside radius and outside radius of the coil respectively, $J_1(\gamma)$ and $J_1(ay)$ are the Bessel functions of first kind, l is the lift-off, h is the height of the coil, μ_1 and σ_1 are the permeability and conductivity of the conductor respectively, and ω is the angular frequency.

An axis-symmetrical geometry, with detailed parameters shown in Table 1, is built to study the analytical solution. Fig. 3(a) illustrates the distribution of the vector potential along the surface of the aluminium plate ($x = 0$); the red[1] square in this curve means the maximum vector potential. From this image, the vector potential is not symmetrical with $y = 5$ mm, where the circular coil is located; that is because the wire of the circular coil is bent.

We proposed a hypothesis, that is, when the radius of the circular coil is large enough, the bent wire of the circular coil can be approximated to a straight wire, and the vector potential should be symmetrical. The model used is the same with the one used in Table 1, with only one difference that the radius of the circular coil is enlarged to 10.04 mm. Fig. 3(b) shows the result of the vector potential distribution for a large-radius coil. The vector potential is now symmetrical with $y = 10.04$ mm; this verifies the hypothesis that, when the radius of the circular coil is very large, the bent wire of the circular coil can be approximated to a straight wire, and the magnitude distribution of the vector potential is symmetrical with the radius [28].

In order to analyse the accuracy of the proposed adapted analytical solutions, the finite element method (FEM) is employed to compare the results between the analytical and the numerical methods. Maxwell Ansoft based on the finite element method (FEM) is used to solve the vector potential; the model built with Maxwell Ansoft is the same with the one built in Fig. 3(b). The computation of the FEM solver is based on minimising the energy error; the vacuum region to be solved is four times as larger as the aluminium plate; the mesh number used is over 7000, which makes the energy error below to 0.1%. The comparison between the analytical method and the finite element method (FEM) is undertaken, not only at a low frequency but also at a high frequency. The comparison results are shown in Fig. 4, revealing that the analytical method shows an accuracy benefit over the finite element method (FEM): the vector potential from the finite element method (FEM) does not approach to zero when it is far away from the wire (Fig. 4(a)–(c)); the curve from the finite element method (FEM) is not smooth at the high frequency, that is due to the numerical nature of the FEM: numerical approximation due to finite mesh density and element interpolation are inevitable.

---

[1] For interpretation of color in Figs. 3 and 9, the reader is referred to the web version of this article.